JOURNAL OF MATERIALS SCIENCE 18 (1983) 1872–1880

# Embrittlement of P/M X7091 and I/M 7175 aluminium alloys by mercury solutions

J. R. PICKENS, W. PRECHT, A. R. C. WESTWOOD
*Martin Marietta Laboratories, Baltimore, Maryland 21227, USA*

This study investigated the embrittlement of aluminium powder metallurgy (P/M) alloy X7091 and the similar ingot metallurgy (I/M) alloy 7175 by liquid mercury ($Hg_L$) and a liquid mercury–gallium solution. The variables examined were duration of pre-test exposure to liquid metal before loading, specimen orientation, grain size and texture, test temperature, and pre-strain before exposure. The liquid metal embrittlement (LME) fracture path was invariably intergranular so grain boundary segregation was measured by Auger electron spectroscopy of specimens pre-exposed to liquid gallium (to induce intergranular failures) that were fractured under high vacuum. The P/M alloy was found to be less susceptible to LME than the I/M alloy. Two embrittlement mechanisms were identified – adsorption-dependent LME and a grain boundary corrosion reaction in which $Hg_L$ dissolves $MgZn_2$ precipitates. P/M X7091 exhibits less grain boundary segregation of magnesium than does I/M 7175, which partially explains the lower susceptibility of the P/M alloy.

## 1. Introduction

The behaviour of metallic alloys in the presence of liquid metals is often unpredictable. For example, the fracture stresses of various aluminium alloys wetted with liquid mercury–zinc solutions first increase in proportion to their ultimate tensile strengths in air until the latter reaches ~ 450 MPa, and then decrease [1]. Polycrystalline pure aluminium fractured in the presence of liquid mercury–gallium solutions undergoes an extremely sharp brittle-to-ductile transition at a temperature, $T_c$, that is a sensitive function of gallium content [2]. In addition, the fracture stress, $\sigma_F$, of annealed Al–Mg alloy 5083 exhibits a typical Petch relationship when wetted with liquid mercury, $Hg_L$ (i.e. $\sigma_F$ increases with $d^{-1/2}$, where $d$ is the mean grain diameter), but follows an *inverse* Petch relationship, $\sigma_F$ decreasing with $d^{-1/2}$, when pre-strained 5% before wetting [3]. Other intriguing examples of the phenomenology of the liquid metal embrittlement (LME) of conventional aluminium alloys have been discussed in various reviews [1, 4–6]. However, to our knowledge, no data have yet been published on the embrittlement behaviour of the emerging powder metallurgy (P/M) alloys.

Aluminium P/M alloys demonstrating excellent combinations of mechanical properties and resistance to environmental attack are now commercially available. One P/M alloy in particular, X7091, exhibits especially attractive combinations of strength, toughness, and resistance to corrosion and stress-corrosion cracking (SCC) [7, 8]. The composition of this Al–Zn–Mg–Cu alloy is similar to that of the ingot metallurgy (I/M) alloy 7175, but it also contains 0.4 wt% Co. Alloy X7091 is made from rapidly solidified powder, and its microstructure is extremely fine-grained and homogeneous. Its aqueous corrosion and SCC behaviour have been studied, but not its susceptibility to LME. This investigation was undertaken to provide an initial survey of the phenomenology of LME for this alloy in $Hg_L$ and in a Hg + 1.5 at% Ga solution ($(Hg + 1.5\,Ga)_L$ hereafter). For comparison, we also studied the LME behaviour of the conventional I/M alloy 7175. Our objectives were to generate baseline data for subsequent mechanistic studies, and to establish if this P/M alloy is relatively more or less vulnerable to LME than an I/M alloy of similar composition. Variables examined were duration of exposure to liquid


0022–2461/83 $03.00 + .12 

TABLE I Chemical composition (wt %) of alloys

| Alloy | Element | | | | | | | | | | | |
|---|---|---|---|---|---|---|---|---|---|---|---|---|
| | Zn | Mg | Cu | Co | Fe | Si | Ni | Mn | Cr | Ti | Zr | Al |
| 7175 | 5.62 | 2.61 | 1.58 | – | 0.16 | 0.07 | 0.01 | – | 0.20 | 0.03 | 0.04 | Balance |
| X7091 | 6.55 | 2.57 | 1.60 | 0.47 | 0.12 | 0.06 | – | – | – | – | – | Balance |
| G | 4.43 | 3.73 | < 0.01 | < 0.01 | < 0.01 | 0.01 | < 0.01 | < 0.01 | < 0.01 | < 0.01 | < 0.01 | Balance |

metal before loading, specimen orientation, grain size and texture, test temperature, strain before exposure, and liquid metal composition.

## 2. Materials and experimental procedure

An extruded P/M X7091 bar (11.4 cm x 3.8 cm in cross-section and of the composition given in Table I) was purchased from Alcoa in the T7E69 (slightly overaged) temper. It was extruded from a ~ 17.1 cm diameter billet at an extrusion ratio of 5.7. Martin Marietta Aluminum supplied the I/M alloy 7175 as a 10.2 cm x 10.2 cm extruded bar in the F (as-fabricated) temper. Its composition also is given in Table I. A coarse-grained, high purity Al–4.43 wt % Zn–3.73 wt % Mg alloy (designated alloy "G") was used to establish wetting parameters and for fractographic studies. This material was purchased from Reynolds Specialty Metals in the form of 0.13 cm thick sheet.

Tensile specimens measuring 7.5 cm or 3.8 cm long and 0.13 cm thick, and having 0.64 cm or 0.32 cm test-section widths, were machined from each alloy in the longitudinal (L), long transverse (LT), and short transverse (ST) orientations. They were heat-treated to peak hardness using the following schedules: X7091 – solution heat-treat for 2 h at (all ± 2° C) 488° C, ice-water quench (WQ), age for 24 h at 121° C, final age for 1 h at 157° C; 7175-T6 – solution heat-treat for 2 h at 482° C, WQ, age 24 h at 123° C; alloy G – solution heat-treat at 475° C, WQ, age 2 h at 120° C. The mean-linear-intercept grain size [9] for each alloy in the L, LT, and ST orientation was determined optically or by transmission electron microscopy. Values in the L, LT, and ST direction were, respectively: X7091 – 2.0 μm x 1.6 μm x 1.6 μm; 7175 – 350 μm x 17 μm x 16 μm; G – 175 μm x 170 μm x 185 μm.

Following heat treatment, all test-section surfaces were polished to a 600-grit finish. Unless otherwise stated, specimens were tested in the LT orientation.

Table II presents the tensile properties of the alloys, tested in air, as a function of orientation.

It was difficult to wet the surfaces of the tensile specimens with mercury, especially the surfaces of the P/M alloy, and the procedure eventually used was to first remove surface oxide films with concentrated HF, and then to apply an approximately 2 ml drop of liquid metal through the acid onto each face of the sheet specimen. The time between wetting and testing (pre-test exposure time; $t_p$ hereafter) was standardized at 5 min, unless otherwise stated.

All specimens were fractured under silicone oil to minimize the tendency for complicating corrosive reactions related to the presence of water vapour in the test environment. The crosshead speed was 0.084 cm $min^{-1}$. Each value of $\sigma_f$ quoted in the following section is the mean of 5 ± 2 tests.

Because fracture of polycrystalline aluminium alloys under mercury [2] or gallium [1, 2, 10, 11] is usually intergranular, it was deemed useful to determine the grain boundary composition by Auger electron spectroscopy (AES). To do this, notched specimens of X7091 and 7175, measuring

TABLE II Mechanical properties of alloys tested in air at room temperature

| Alloy | Heat treatment | Orientation | 0.2% offset yield strength (MPa) | UTS (MPa) | Elongation (%) |
|---|---|---|---|---|---|
| 7175 | T6 | L | 503 | 552 | 5.0 |
| | | LT | 490 | 545 | 8.1 |
| | | ST | 469 | 531 | 8.3 |
| X7091 | Peak hardness | LT | 552 | 586 | 7.5 |
| | | ST | 483 | 524 | 6.0 |
| G | Peak hardness | L* | 276 | 338 | 10.2 |

*Orientation is of minor importance because this alloy exhibited a recrystallized, equiaxed structure.

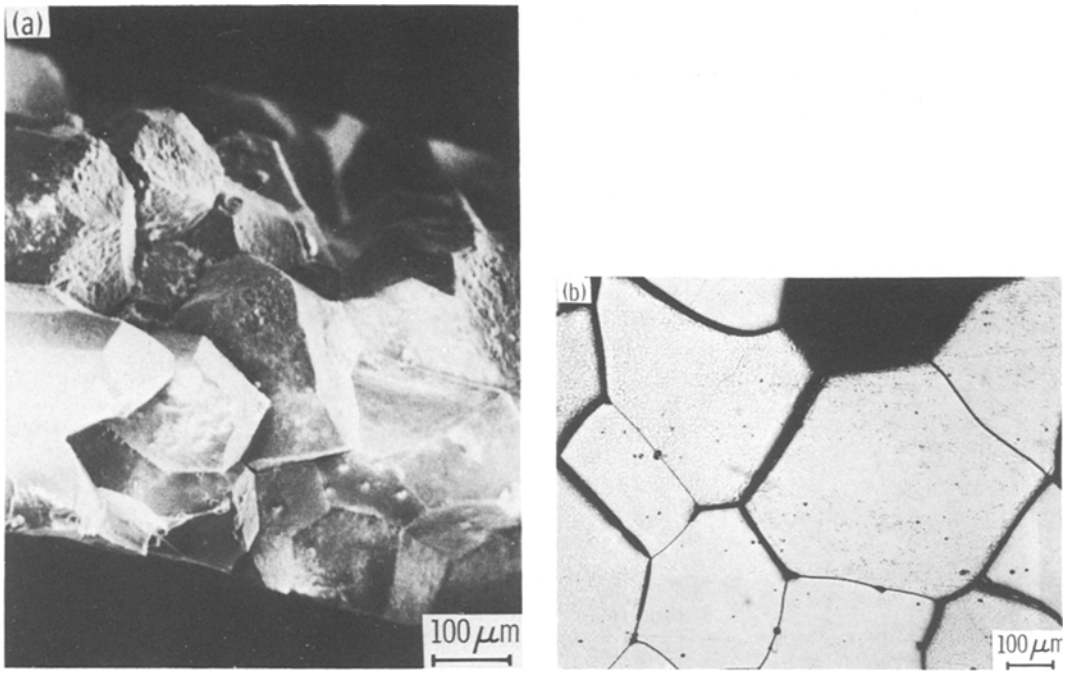


*Figure 1* (a) Fracture surface and (b) fracture surface profile of alloy G fractured under $Hg_L$ showing the intergranular nature of the embrittlement.

2.5 cm x 3.2 cm x 0.13 cm, were fractured under ultra-high vacuum in the Auger spectrometer chamber. Fracture of polycrystalline aluminium alloys at liquid nitrogen temperatures (− 194° C) has been assumed to proceed along the grain boundary plane [12, 13] and several were fractured at this temperature to expose the grain boundaries. To ensure grain boundary fracture, several specimens of each alloy were pre-exposed to $Ga_L$ at 35° C for 4 h prior to fracture in the Auger chamber at room temperature. The energies of two Auger peaks for gallium (985 and 1001 eV) are very similar to the major peak for zinc, 994 eV, so zinc segregation is difficult to measure. Accordingly, the magnesium to aluminium peak-to-peak ratio (Mg/Al hereafter) was used as a measure of grain boundary segregation.

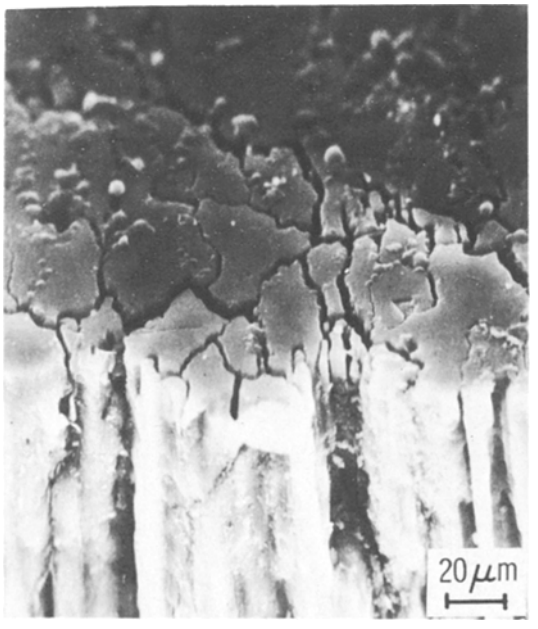


*Figure 2* Intergranular LME in 7175.

## 3. Results and discussion

Specimens tested in the liquid metal environments showed no measurable ductility, so values of $\sigma_F$ alone were used to evaluate relative degrees of embrittlement.

The fracture path was intergranular for all three alloys (see Figs. 1 to 3). I/M 7175 alloy was more sensitive to pre-test exposure time, $t_p$, than was the P/M X7091 alloy (see Table III). Values of $\sigma_F$ for 7175 were markedly lower for both $Hg_L$ and $(Hg + 1.5\ Ga)_L$ environments when $t_p$ was 60 min instead of 5 min (Table III). In contrast, $\sigma_F$ for X7091 was similar for both values of $t_p$ for $Hg_L$, and decreased moderately with $t_p$ for $(Hg + 1.5\ Ga)_L$.

Ichinose [14] found that $\sigma_F$ for pure aluminium wetted with $Hg_L$ is independent of $t_p$.

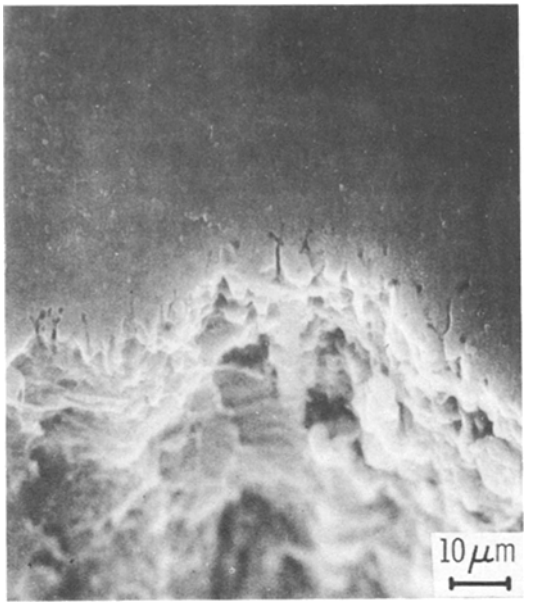


*Figure 3* Predominantly intergranular LME in X7091.

Thus, the observation that $\sigma_F$ for 7175 generally decreases with exposure time for both $Hg_L$ and $(Hg + 1.5\ Ga)_L$ environments (Table III) suggests that some phenomenon other than stress-dependent LME is operating. It is known that gallium readily penetrates the grain boundaries of aluminium alloys [4, 10, 11], so a reduction in $\sigma_F$ with $t_p$ for the $(Hg + 1.5\ Ga)_L$ environment can be anticipated on this basis. Mercury on the other hand tends not to penetrate clean aluminium grain boundaries, so the variation of $\sigma_F$ with $t_p$ for the 7175 specimens wetted with $Hg_L$ suggests that boundary composition, and possibly the presence of intermetallic phases, might also be an important variable in the embrittlement process. To examine this possibility, metallographic and corrosion studies were conducted. Microstructural examination of wetted

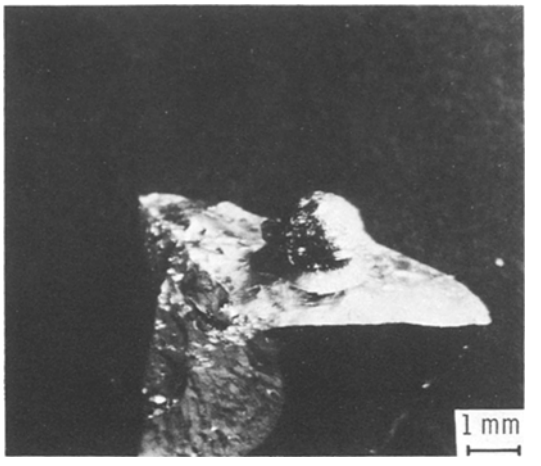


*Figure 4* Amalgam formed by reaction between $Hg_L$ droplet and $MgZn_2$ crystal.

boundary regions revealed that an amalgam phase was formed in the boundary region of each of the three alloys. This was most evident for alloy G (see Fig. 1). The composition of the amalgam was determined by atomic absorption to be ~ 45 wt % Zn, 8.5 wt % Mg, and 45.5 wt % Hg. The wt % ratio of zinc to magnesium in the amalgam is 5.29 – very close to that of 5.37 for $MgZn_2$, a phase known to precipitate at grain boundaries in Al–Zn–Mg alloys. This implies that $MgZn_2$ and similar precipitates may be dissolved by the liquid mercury.

To investigate this possibility, a droplet of $Hg_L$ was placed on the surface of a stoichiometric monocrystal of $MgZn_2$. A vigorous reaction occurred, and a dark amalgam phase was formed within a few seconds (see Fig. 4). Thus, it appears likely that grain boundary "corrosion" involving intermetallic precipitates occurs in Al–Zn–Mg alloys, and that this effect is responsible for the time dependence of $\sigma_F$ when they are wetted with $Hg_L$.

TABLE III Effect of pre-test exposure time ($t_p$) and liquid metal environment on fracture stress, $\sigma_F$, at 25° C (LT orientation)

| Alloy | Heat treatment | $t_p$ (min) | Liquid metal | Fracture stress, $\sigma_F$ (MPa ± standard deviation) |
|---|---|---|---|---|
| X7091 | Peak hardness | 5 | Hg | 135 ± 13 |
| X7091 | Peak hardness | 60 | Hg | 131 ± 20 |
| X7091 | Peak hardness | 5 | Hg + 1.5 Ga | 119 ± 12 |
| X7091 | Peak hardness | 60 | Hg + 1.5 Ga | 94 ± 25 |
| 7175 | T6 | 5 | Hg | 80 ± 15 |
| 7175 | T6 | 60 | Hg | 15 ± 9 |
| 7175 | T6 | 5 | Hg + 1.5 Ga | 68 ± 17 |
| 7175 | T6 | 60 | Hg + 1.5 Ga | 22 ± 6 |

TABLE IV Grain boundary composition as determined by Auger electron spectroscopy

| Alloy | Specimen number | Pre-exposure | Mg/Al |
|---|---|---|---|
| 7175-T6 (LT) | 1 | no | 0.05 |
| | 2 | no | 0.36 |
| | 3 | no | 0.12 |
| | 4 | Ga | 1.5 |
| | 5 | Ga | 1.9 |
| X7091-Peak (LT) | 1 | no | 0.10 |
| | 2 | no | 0.13 |
| | 3 | Ga | 0.33 |
| | 4 | Ga | 0.24 |

TABLE V Effect of specimen orientation on fracture stress in $Hg_L$ at 25° C

| Alloy | Orientation | Wetting time (min) | Fracture stress, $\sigma_F$ (MPa ± standard deviation) |
|---|---|---|---|
| 7175 | ST | 5 | 60 ± 15 |
| | LT | 5 | 80 ± 15 |
| | L | 5 | 220 ± 40 |
| | ST | 60 | 10 ± 1 |
| | LT | 60 | 15 ± 9 |
| X7091 | ST | 5 | 60 ± 20 |
| | LT | 5 | 135 ± 13 |
| | L | 5 | > 260 ± ~ 20 |

The amalgam that formed on the $MgZn_2$ monocrystal expanded during formation. This expansion may contribute to embrittlement, as evidenced by entire grains falling out of specimens of alloy G wetted with $Hg_L$, in the absence of an applied stress. The dentistry literature notes that many amalgams exhibit dimensional instability upon formation and ageing [15]. For example, solutions of zinc in $Hg_L$ expand both on formation and for several days thereafter [16].

The more pronounced effect of $t_p$ on $\sigma_F$ in 7175 than in X7091 may be related to the much greater grain boundary area-to-volume ratio of the latter. Perhaps this causes boundary segregation to be less severe in the P/M alloy and, consequently, the contribution of the corrosion reaction to embrittlement is less.

Attempts to measure the degree of boundary segregation in 7175 fractured at $-194°$ C using AES produced scattered results (Table IV). Pre-exposure to $Ga_L$ reduced scatter, and markedly increased the Mg/Al ratio. This may mean that fracture does not proceed precisely along grain boundary planes in specimens that are not pre-exposed, instead propagating at least partially through the precipitate-free zone.

Magnesium segregation in X7091 pre-exposed to $Ga_L$ was roughly one-fifth of that in 7175 (see Table IV). The magnesium content measured presumably includes magnesium in grain boundary precipitates as well as "free magnesium" that segregates to the grain boundary [12, 17]. Unfortunately, because the Auger peak for zinc was obscured by those of gallium in embrittled specimens, meaningful data on its segregation could not be obtained. On the other hand, it does appear from Table IV that the segregation of magnesium is more severe in 7175 than in X7091, a finding consistent with the hypothesis above and explaining the greater effect of $t_p$ on $\sigma_F$ in 7175 than in X7091.

### 3.1. Effect of specimen orientation

For both alloys, L-oriented specimens were less susceptible to LME than were LT specimens, and these, in turn, were less susceptible than ST specimens (see Table V). This orientation dependence is also characteristic for other embrittlement phenomena, such as SCC and hydrogen embrittlement (HE). In these cases, this effect is usually interpreted as follows: the grain texture provides the least circuitous crack path in the ST orientation, a more circuitous path in the LT, and the most circuitous path in the L orientation. In the present work, however, the microstructure of the X7091 alloy is roughly equiaxed, so some other factor must be responsible for the differences observed in this case.

One possibility is that prior (powder) particle boundaries (PPBs) may develop a preferred orientation during extrusion that is maintained through subsequent recrystallization events. Thus, LME may proceed, in part, along PPBs. To investigate this possibility, we used scanning electron microscopy (SEM) to examine the fracture surfaces of X7091. Fractographic features elongated in the extrusion direction (see Fig. 5) of dimensions expected for PPBs (extrusion ratio = 5.7:1) were noted. However, transmission electron microscopy (TEM) studies using various imaging conditions failed to reveal specific PPBs. Apparently, surface oxides were well broken up during extrusion and were distributed fairly uniformly throughout the microstructure. Thus, the origin of the orientation-dependence of $\sigma_F$ for X7091 is not yet clear.

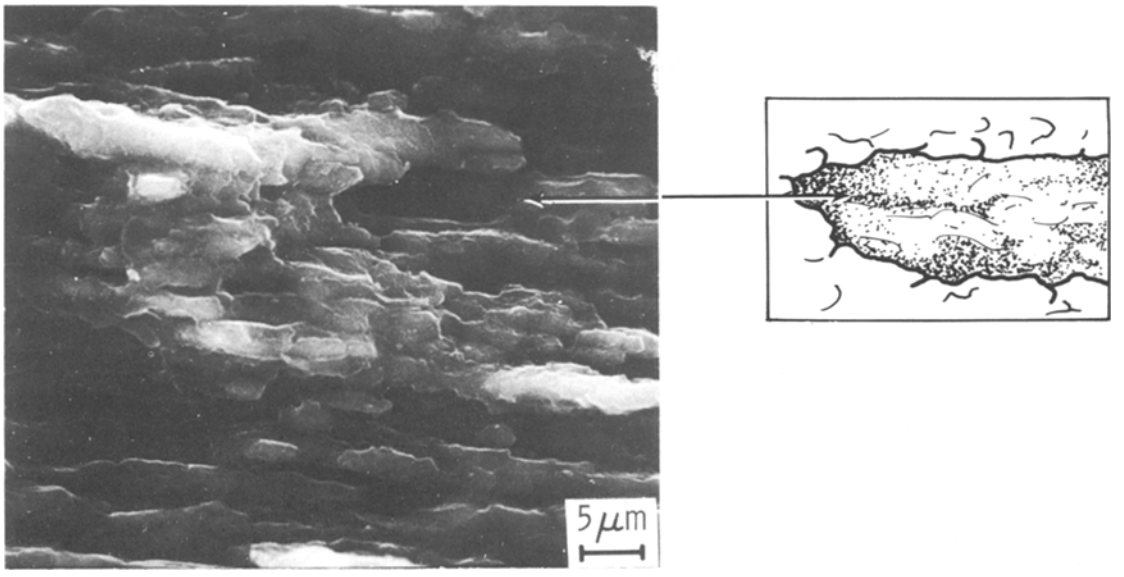


*Figure 5* SEM fractograph of X7091. Some fractographic features are approximately the size expected for the prior powder particles.

### 3.2. Effect of temperature

The particular batch of X7091 specimens used for this experiment was inadvertently overaged slightly and were not as strong as the 7175 specimens.

The temperature sensitivity of embrittlement is illustrated in Fig. 6. $\sigma_F$ for X7091 under $Hg_L$ and $(Hg + 1.5\ Ga)_L$ first decreased slightly with temperature over the range of $-30$ to 60° C, and then gradually increased as the temperature was raised from 60 to 200° C. For 7175, $\sigma_F$ remained at a relatively constant, low value from 0 to 200° C.

Note that the increase in $\sigma_F$ for X7091 occurred over a broad temperature range, and was not as abrupt as other researchers have noted for pure aluminium in $Hg_L$ [2]. A possible explanation for this difference may be offered in terms of the schematic in Fig. 7. When adsorption-dependent LME is the only embrittlement phenomenon involved, a rather sharp brittle-to-ductile transition is usually observed. However, for alloys in which grain boundary corrosion is also significantly involved, e.g. 7175, the rate and influence of corrosion increases with temperature – thus accounting for the limited or non-restoration of ductility with increasing temperature. A similar effect occurs when pure aluminium is tested in $Ga_L$ [2]. For X7091, boundary corrosion is less involved and so, as expected, an intermediate temperature dependence is observed.

It is possible that the dependence of the temperature of brittle-to-ductile transitions, $T_c$, on grain size often observed may be used to interpret the behaviour illustrated in Fig. 6. The Petch [18] relationship, $T_c \propto \ln d$, predicts a lower $T_c$ for the finer-grained X7091 than for 7175, so perhaps

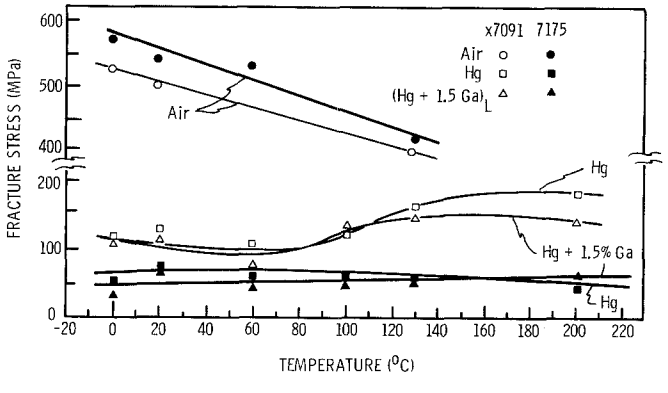


*Figure 6* Variation in fracture stress with test temperature in various environments.

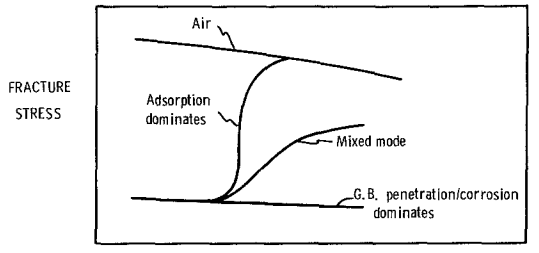


*Figure 7* Schematic of possible explanations for observed dependence of fracture stress on temperature.

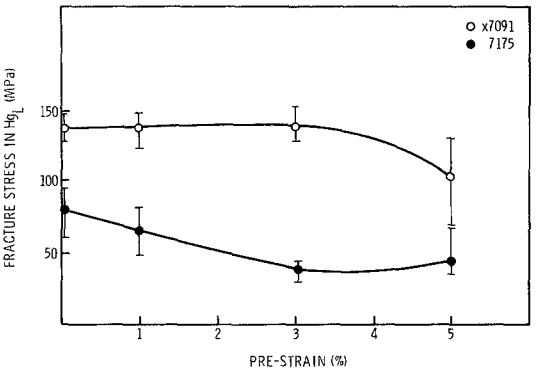


*Figure 8* Effect of straining prior to wetting on fracture stress.

$T_c$ for 7175 is above 200° C, the highest temperature studied. On the other hand, Ichinose and Oouchi [19] have noted that $T_c$ increases as grain size is reduced for pre-strained aluminium wetted with $(Hg–3Zn)_L$ – an observation that is not consistent with the trend we observe. More work is needed on this point.

### 3.3. Effect of pre-strain

Pre-straining up to 5% prior to wetting affected fracture stress as shown in Fig. 8. $\sigma_F$ for X7091 remained relatively constant up to 3% pre-strain, then decreased, while $\sigma_F$ for 7175 decreased for pre-strains of up to 3%, then stayed essentially constant. Presumably, these modest amounts of pre-strain reduced $\sigma_F$ in the embrittling environment by providing pre-existing obstacles to slip that facilitated fracture.

### 3.4. Effect of grain size

Susceptibility to embrittlement increased with grain size for the three alloys tested (X7091 < 7175 < G). Alloy G, having the largest grain size, was most severely embrittled, literally disintegrating seconds after liquid mercury was applied.

The finding that susceptibility to LME increases with grain size for the three alloys used – although they are of slightly different chemical compositions – is consistent with the findings of Ichinose and Oouchi [20]. This effect is amplified for the materials used here because of the marked contribution to embrittlement of corrosion in the larger-grained alloys.

### 3.5. Effect of composition of the liquid metal environment

Embrittlement in $(Hg + 1.5\,Ga)_L$ environments was generally more severe than that in $Hg_L$ (see Table III and Fig. 6), as previously established for aluminium alloys [2], and the increase is attributed to gallium diffusion into, and embrittlement of, the grain boundaries [2, 10, 11].

Specimens of X7091 and 7175 stressed while immersed in $Hg_L$, but without particular care being taken to ensure wetting, fractured at stresses much higher than those obtained when the oxide film was removed with HF prior to exposure to $Hg_L$. Values of 380 MPa were obtained for X7091 and 400 MPa for 7175. This implies that surface oxide films did not fracture sufficiently to permit $Hg_L$ ready access to the substrate aluminium at stresses below ~ 70% of the yield stress of the alloys.

### 3.6. Other comments

Auger depth profiling revealed essentially identical compositions and thicknesses of natural oxide films on I/M 7175 and P/M X7091 alloys (see Fig. 9). Both films are ~ 5.0 nm thick, and consist predominantly of aluminium oxide. The carbon profile results from contamination. The similarity in nature of the oxide films is consistent with the comparable fracture stresses observed when unprepared (i.e. no HF) specimens of each alloy are tested in $Hg_L$. The greater ease of wetting oxide-free 7175 than X7091 is probably related to enhanced boundary segregation in the former alloy. We suspect that after the oxide films are removed by HF, $Hg_L$ wets grain boundary regions having extensive $MgZn_2$ precipitation, which are more common in the 7175.

## 4. Conclusions

On the basis of this study, it appears that:

1. The P/M alloy X7091 is less susceptible to embrittlement by $Hg_L$ or $(Hg + 1.5\,Ga)_L$ than is the I/M alloy 7175.

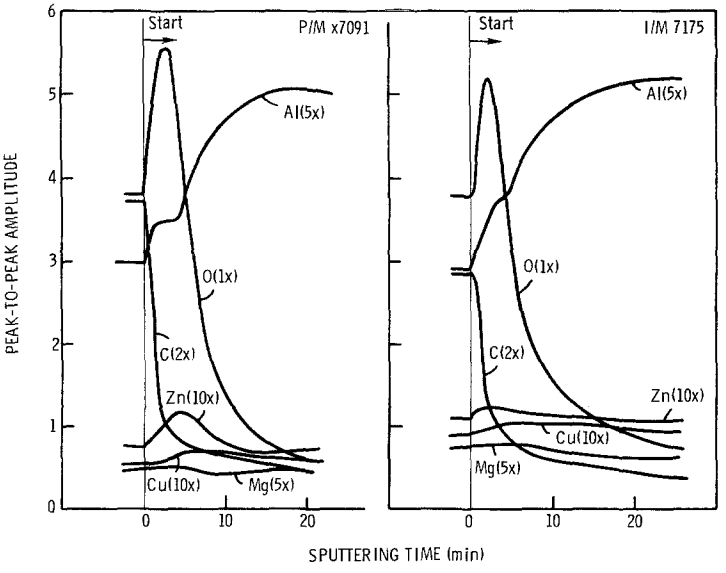


*Figure 9* Auger depth profiles of surface oxide films formed after mechanical polishing. The carbon profiles result from contamination in the Auger chamber. Sputtered at 0.8 nm $min^{-1}$.

2. Two embrittlement mechanisms are involved when Al–Zn–Mg alloys are wetted with mercury solutions: adsorption-dependent LME and grain boundary corrosion. The latter probably involves a reaction between $Hg_L$ and $MgZn_2$ precipitates at the boundaries.

3. X7091 exhibits less grain boundary segregation of magnesium than does 7175, and this factor probably contributes to its relatively decreased susceptibility.

4. Fracture in $Hg_L$ and $(Hg + 1.5\,Ga)_L$ was intergranular in all cases, and susceptibility to embrittlement increased with grain size.

5. Segregation effects can play an important role in intergranular LME.

6. Although the surface oxide films on both X7091 and 7175 make these alloys difficult to wet by $Hg_L$ and $(Hg + 1.5\,Ga)_L$, the alloys are potentially vulnerable to catastrophic failure when loaded to high stresses in mercury environments.

## Acknowledgements

We greatly appreciate the useful discussions with W. S. Cebulak, L. Christodoulou, S. P. Lynch and R. M. Latanision; the technical assistance of R. Butler, V. Farber, and most of all L. Colton. We are particularly grateful to G. D. Davis for his insights in interpreting the Auger data. This work was supported by the National Science Foundation under Grant No. DMR-80-13457.

## References

1. W. ROSTOKER, J. M. McCAUGHEY and J. MARKUS, "Embrittlement by Liquid Metals" (Reinhold, New York, 1960) pp. 28, 61.
2. C. M. PREECE and A. R. C. WESTWOOD, *Trans. Amer. Soc. Met.* **62** (1969) 418.
3. H. NICHOLS and W. ROSTOKER, *Trans. AIME* **224** (1963) 1258.
4. A. R. C. WESTWOOD, C. M. PREECE and M. H. KAMDAR, in "Fracture: An Advanced Treatise", edited by H. Liebowitz (Academic Press, New York, 1971) pp. 589–644.
5. N. S. STOLOFF, in "Environment Sensitive Fracture in Engineering Metals" (Metallurgical Society of AIME, New York, 1979) pp. 486–518.
6. *Idem*, in "Atomistics of Fracture", edited by R. M. Latanision and J. R. Pickens (Plenum Press, New York, 1982). pp. 921–46.
7. W. S. CEBULAK, E. W. JOHNSON and H. MARKUS, *Int. J. Powder Metall. Powder Tech.* **12** (1976) 299.
8. R. M. HART, "Wrought P/M Aluminum Alloys X7090 and X7091", August 1981, Alcoa Green Letter, Aluminum Company of America.
9. E. E. UNDERWOOD, "Quantitative Stereology" (Addison-Wesley Publishing Co., Reading, MA, 1970) pp. 34, 81, 82.
10. C. ROQUES-CARMES, M. AUCOUTURIER and P. LACOMBE, *Met. Sci. J.* 7 (1973) 128.
11. S. K. MARYA and G. WYON, *Scripta Metall.* **9** (1975) 1009.
12. T. S. SUN, J. M. CHEN, R. K. VISWANADHAM and J. A. S. GREEN, *Appl. Phys. Lett.* **31** (1977) 580.
13. A. JOSHI, C. R. SHASTRY and M. LEVY, *Met. Trans. A* **12A** (1981) 1081.
14. M. ICHINOSE, *Trans. Jpn. Inst. Met.* **7** (1966) 57.
15. G. C. PAFFENBARGER, N. W. RUPP and P. R. PATEL, *J. Amer. Dent. Assoc.* **99** (1979) 468.
16. R. W. PHILLIPS, "Skinner's Science of Dental Materials" (W. B. Saunders Co., Philadelphia, 1973) pp. 335–365.
17. R. K. VISWANADHAM, T. S. SUN and J. A. S.

GREEN, *Met. Trans. A* **11A** (1980) 85.
18. N. J. PETCH, "Fracture, Proceedings of Swampscott Conference" (John Wiley and Sons, New York, 1959).
19. H. ICHINOSE and C. OOUCHI, *Trans. Jpn. Inst. Met.* **9** (1968) 980.
20. *Idem, ibid.* **9** (1968) 41.

*Received 1 November*
*and accepted 23 November 1982*